Direct Numerical Analysis of Dynamic Facilitation in Glass-Forming Liquids

Cecilia Herrero[1] and Ludovic Berthier[1,2,*]
[1]Laboratoire Charles Coulomb (L2C), Université de Montpellier, CNRS, 34095 Montpellier, France
[2]Gulliver, UMR CNRS 7083, ESPCI Paris, PSL Research University, 75005 Paris, France

(Received 8 November 2023; accepted 21 May 2024; published 21 June 2024)

We propose a computational strategy to quantify the temperature evolution of the timescales and length scales over which dynamic facilitation affects the relaxation dynamics of glass-forming liquids at low temperatures, which requires no assumption about the nature of the dynamics. In two glass models, we find that dynamic facilitation depends strongly on temperature, leading to a subdiffusive spreading of relaxation events which we characterize using a temperature-dependent dynamic exponent. We also establish that this temperature evolution represents a major contribution to the increase of the structural relaxation time.

DOI: 10.1103/PhysRevLett.132.258201

The relaxation dynamics of glass formers in the vicinity of the experimental glass transition is not fully elucidated [1–3]. It is often difficult to draw firm conclusions about the relative role of distinct mechanisms from measurements without relying on unproven hypothesis [4]. Our main goal is to quantitatively assess the role and temperature evolution of dynamic facilitation [5–8] in the relaxation of glass-forming liquids without making assumptions about the nature of relaxation events.

Dynamic facilitation captures the physical idea that a relaxation event happening somewhere causally triggers future relaxation events. It is invoked in several theoretical approaches [9–11]. Some models and theories are directly constructed around facilitation [6–8,12], thought to be triggered by localized mobility defects. It has been suggested that elasticity may be responsible for mediating dynamic information [10,13–15]. However, there exists no first-principles description of dynamic facilitation to predict its strength and temperature evolution for atomistic models.

Progress will require quantitative observations from realistic models. Previous work suggested the existence of dynamic facilitation by detecting cross-correlations between successive relaxation events [16–20], but this approach remains qualitative. In [18,21,22], the relaxation dynamics was deemed hierarchical, which amounts to the logarithmic growth of energy barriers with distance. Invoking the Arrhenius law, this is mathematically equivalent to a power-law relation between timescales and length scales, $t \sim \ell^z$, with a temperature-dependent dynamic exponent, $z(T) \sim 1/T$, as explicitly found in certain kinetically constrained models [7,23,24].

The large body of data accumulated in studies of four-point correlations [25–28] for dynamic heterogeneity [29] can potentially elucidate the relation between space and time [24]. However, their interpretation is not unique [27], as multipoint functions do not directly probe the underlying relaxation mechanisms. At times shorter than the structural relaxation, this problem was circumvented by introducing a growing length scale characterizing the subdiffusive spreading of mobile regions [30].

The emergence of propagating fronts in ultrastable glasses heterogeneously transforming into supercooled liquids [31,32] is a form of dynamic facilitation [33,34], but the nonequilibrium nature of the relaxation leads to a ballistic ($\ell \propto t$) growth of relaxed regions [35], unlike the subdiffusion found in equilibrium.

Here we propose a computational strategy to understand if and how much dynamic facilitation affects the equilibrium dynamics of deeply supercooled liquids. We conduct simulations where a macroscopic interface separates two regions evolving with distinct equilibrium dynamics at the same temperature T: ordinary molecular dynamics (MD) in one domain, and swap Monte Carlo (SMC) dynamics in the other. The rationale is that in bulk dynamics [Fig. 1(a)], rare mobile regions appear whose spatial spreading reveals facilitation [30]. Here instead, SMC dynamics creates a macroscopic mobile region whose influence then spreads to the MD region by facilitation in a controlled geometry [Fig. 1(a)]. Since both regions are equilibrated at the same T, they are structurally indistinguishable at any time and the system is stationary. Therefore, the fast dynamics in the SMC region facilitates relaxation in the MD region. The observed relaxation is representative of the equilibrium dynamics, but the measurement of a macroscopic mobility front [Fig. 1(b)] does not rely on any assumption about the nature of the microscopic events or on detailed knowledge of the origin of facilitation. This allows us to directly access the relation between space and time over a broad range of temperatures [Fig. 1(c)].

We perform simulations in two and three dimensions of soft size-polydisperse spheres [41,42], with the same size polydispersity $\delta = 23\%$ (see Supplemental Material [36]). The pairwise interaction potential is

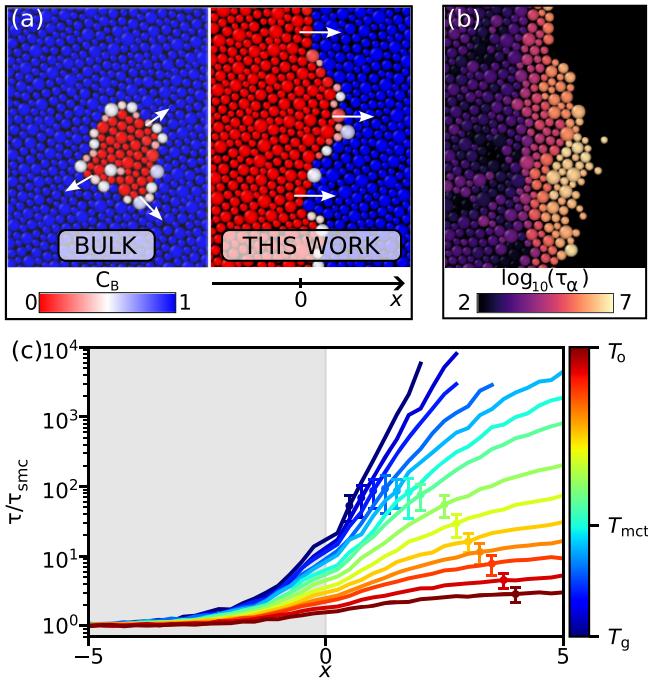

FIG. 1. Direct measurement of dynamic facilitation. (a) Instead of measuring the growth of rare mobile regions in the bulk (left), we create a macroscopic interface (right) separating a mobile region for $x < 0$ (using swap MC) from a region at $x > 0$ where conventional MD at the same T is used. The system is structurally homogeneous at all times. (b) Map of local relaxation times near $x = 0$ showing the spatial spreading of mobility along the horizontal axis ($T = 0.09$). (c) Dynamic profiles showing the evolution of the structural relaxation with x, normalized by $\tau_{\rm smc}$, for the two-dimensional system. Dynamic facilitation becomes less efficient at lower T. Typical error bars are shown at some selected data point for each temperature. Full error bars are shown in the Supplemental Material [36].

$$V_{ij}(r_{ij}) = \varepsilon\left(\frac{\sigma_{ij}}{r_{ij}}\right)^{12} + c_0 + c_2\left(\frac{r_{ij}}{\sigma_{ij}}\right)^2 + c_4\left(\frac{r_{ij}}{\sigma_{ij}}\right)^4, \quad (1)$$

where r_{ij} is the interparticle distance and $\sigma_{ij} = [(\sigma_i + \sigma_j)/2](1 - \eta|\sigma_i - \sigma_j|)$, with $\eta = 0.2$ a nonadditivity parameter. The parameters $c_0 = -28\varepsilon/r_c^{12}$, $c_2 = 48\varepsilon/r_c^{14}$, and $c_4 = -21\varepsilon/r_c^{16}$, ensure the continuity of the potential up to its second derivative at the cutoff distance $r_c = 1.25\sigma_{ij}$. We use reduced units based on the particle mass m, the energy scale ε, and the average particle diameter σ, so the time unit is $\tau = \sigma\sqrt{m/\varepsilon}$.

We first equilibrate the entire system at the desired temperature T and number density $\rho = 1$ using swap Monte Carlo [42–44]. We then impose two distinct dynamics in two regions of space, keeping the periodic boundary conditions. For $x < 0$ we run SMC using the hybrid scheme developed in [44]. For $x > 0$, we run standard molecular dynamics. Because of the periodic boundary conditions the mobile SMC region forms a slab. As rationalized below, we found it convenient to impose SMC on 25% of the system, and MD in the rest. Simulations are performed at constant T using a Nosé-Hoover thermostat with a time step of 0.01. We also varied the amount of swap MC moves [44] for $x < 0$ to assess its role in the quantification of dynamic facilitation. Additional details and several tests are provided in Supplemental Material [36].

We adopt the usual definitions of characteristic temperature scales [30]. In three dimensions, the onset temperature is $T_o = 0.2$, the mode coupling crossover $T_{\rm mct} = 0.095$, and the glass transition temperature $T_g = 0.056$. The total number of particles is $N = 96\,000$ and we explored temperatures in the range $T \in [0.075, 0.2]$. In two dimensions, $T_o = 0.2$, $T_{\rm mct} = 0.12$, $T_g = 0.07$, and we explored temperatures $T \in [0.07, 0.2]$. The number of particles for $T \geq 0.1$ is $N = 10\,000$. For lower T, the relaxation timescale in the MD region is so large that mobility far from the interface is negligible. For $T < 0.1$, we thus simulated a smaller system with $N = 2500$ reducing only the length of the MD region. When possible, we checked that the two geometries provide similar results. We run simulations up to $t = 2 \times 10^7$ (about 2 weeks of CPU time), and perform up to 50 independent simulations per temperature.

We use the bond-breaking correlation to quantify the dynamics:

$$C_B^i(t) = \frac{n_i(t|0)}{n_i(0)}, \quad (2)$$

with $n_i(t)$ the number of neighbors of particle i at time t, and $n_i(t|0)$ the number of those initial neighbors that remain at time t. We follow [45] for the neighbor definitions. At $t = 0$, the neighbors of particle i are particles j, which are closer than a threshold, $r_{ij}/\sigma_{ij} < 1.35$ in two dimensions and $r_{ij}/\sigma_{ij} < 1.49$ in three dimensions, which correspond to the first minima of the rescaled radial distribution function $g(r/\sigma_{ij})$. We spatially resolve the dynamics by measuring $C_B(x, t)$ for all particles in the interval $x \pm \delta x/2$, with $\delta x = 0.25$. We define the relaxation time $\tau(x, T)$ as $C_B(x, \tau) = 0.7$. We obtained equivalent results for different thresholds. We denote $\tau_{\rm smc}$ and τ_α the bulk relaxation times for SMC and MD dynamics, respectively.

Dynamic facilitation is demonstrated in Fig. 1(b), where a gradient of relaxation times is observed near the macroscopic interface at $x = 0$, showing that the mobile regions at $x < 0$ indeed trigger the relaxation of particles following the conventional MD dynamics at $x > 0$. Because the structure is completely homogeneous along x at all times (see Supplemental Material [36]), this acceleration necessarily results from dynamic facilitation. Dynamic profiles $\tau(x, T)$ are reported in Fig. 1(c), using $\tau_{\rm smc}$ as normalization. These data reveal that the spatial spreading of mobility becomes less efficient, and thus much slower, at lower

temperature. See Supplemental Material [36] for an equivalent observation in three dimensions.

Normalizing the data by $\tau_{\rm smc}$ simply shifts the data vertically by an amount $\tau_{\rm smc}$, which depends on the details of the swap Monte Carlo simulations. We have run simulations changing the parameters of the SMC dynamics, and confirmed that the normalized profiles $\tau(x,T)$ are unchanged, see Supplemental Material [36]. When T is not too low we can observe plateaus in both regions when $|x| \gg 1$. In particular, convergence to the MD plateau occurs for $x \sim \xi_d$, where $\xi_d(T)$ is the dynamic correlation length [46]. At low temperatures, τ_α becomes too large and we cannot follow the profiles up to τ_α in the MD region. Crucially, however, since relaxation remains fast in the SMC region, we can still characterize dynamic facilitation over several decades in time down to T_g.

To quantify these observations, we describe for $0 < x < \xi_d$ subdiffusive spreading of mobility from fast to slow regions using either a power law,

$$x \sim \tau(x,T)^{1/z(T)}, \tag{3}$$

where $z(T)$ is a temperature dependent dynamic exponent, or a thermally activated logarithmic form:

$$x \sim T \log \tau(x,T). \tag{4}$$

For $x \approx \xi_d$, we expect a saturation to τ_α, which we capture using

$$\tau(x,T) \sim \tau_\alpha (1 - e^{-x/\xi_d}). \tag{5}$$

In practice, we account for the crossover to $\tau_{\rm smc}$ at $x < 0$ using the expression $\tau(x)/\tau_{\rm smc} = 1 + a(T)(x + x_0)^{z(T)}$, where a, x_0, and $z(T)$ are fitting parameters. This reduces to Eq. (3) in the relevant regime $\tau_{\rm smc} \ll \tau(x,T) \ll \tau_\alpha$. We found that fixing $x_0 = 3.3$ in two dimensions and $x_0 = 3.4$ in three dimensions described the data well. The quality of the fits can be appreciated in Supplemental Material [36]. The temperature evolution of a and z are shown in Figs. 2(a) and 2(b) using the rescaled axis T_o/T to compare both two- and three-dimensional models. We first notice the very comparable evolution obtained for the two models, which reveals the weak influence of the spatial dimension. The temperature evolution of a mostly mirrors the one of $\tau_{\rm smc}$, as it should. The most interesting observation is the evolution of $z(T)$ which reveals nearly diffusive behavior ($z \sim 2$) near T_o, but increases very fast as T is lowered reaching the large value $z \approx 12$ near T_g in two dimensions. The rapid growth of $z(T)$ captures the evolution of dynamic facilitation towards much slower mobility propagation at low temperatures. Our data are compatible with $z(T) \approx A/T$ at low T, with A some constant. The agreement with the single data point reported in Ref. [30], determined in the bulk geometry for the same two-dimensional model, is

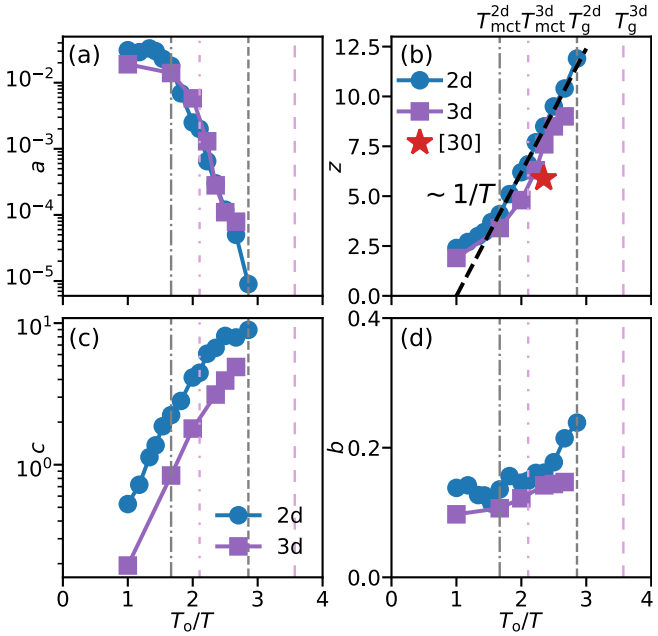

FIG. 2. Temperature evolution of space-time relation. Evolution of fitting parameters in two- and three-dimensional models. (a),(b) Parameters for power law fit. The red star in (b) corresponds to the measurement in Ref. [30], and the black dashed line to a $z \sim 1/T$ behavior. (c),(d) Parameters for logarithmic growth.

quite good, given the difference in methodologies. We also characterized the growth of isolated domains directly in the bulk (see Supplemental Material [36]), and found good agreement with the $z(t)$ results reported in Fig. 2(b). This provides quantitative support to the analogy between the geometries illustrated in Fig. 1(a).

Given the large values of z, it is natural that a logarithmic growth can also be used, although the linear behavior predicted in Eq. (4) is not obvious in the profiles shown in Fig. 1(c). In practice, we fit the data to the functional form $\tau(x,T)/\tau_{\rm smc} = 1 + c(T)\exp[b(T)x/T]$ with c and b fitting parameters. This expression reduces to Eq. (4) far from the plateaus. This second form fits a slightly smaller x range but describes the evolution of the dynamic profiles reasonably well, as shown in Supplemental Material [36]. We report the mild, but non-negligible, evolution of the parameters b and c in Figs. 2(c) and 2(d) which again reveal a similar evolution for both models. It is not surprising that both power-law and logarithmic functional forms can fit the data at low temperatures, as they are mathematically close when $z(T) \approx A/T$ since $x \sim \tau^{1/z(T)} = e^{(T/A)\log\tau} \sim 1 + (T/A)\log\tau$. This coincidence was noted before [47,48].

We finally use Eq. (5) to extract the dynamic correlation length scale ξ_d. At very low temperatures where the MD plateau cannot be reached, we use an extrapolation of the bulk relaxation times $\tau_\alpha(T)$ using a parabolic law [49]. We then estimate ξ_d from the fit to the dynamic profile, assuming $\tau(x = \xi_d, T) = \tau_\alpha(T)$. We verified that both

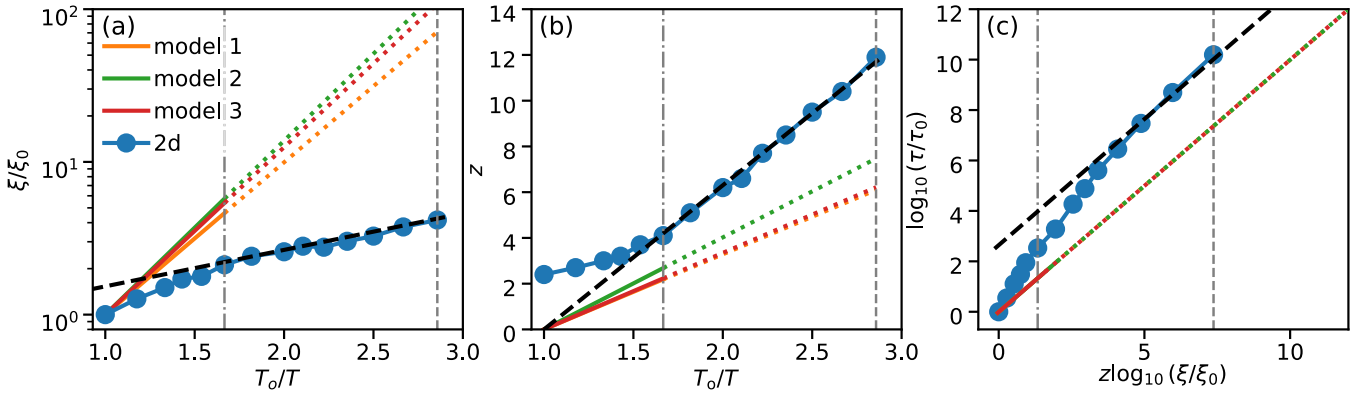

FIG. 3. Understanding the temperature evolution of structural relaxation. Simulation results for the two-dimensional system (circles), compared to results for three different models from Ref. [18] (full lines are actual results, dotted lines are continuation to T_g using asymptotic expressions). (a) Dynamic correlation length ξ_d normalized by its onset value as a function of T_o/T. Black dashed line is an Arrhenius fit. (b) Dynamic exponent z as a function of T_o/T. Black dashed line is $z(T) \sim A/T$. (c) Parametric plot of τ_α against its facilitation estimate ξ_d^z. Black dashed line indicates linear relation, which leaves an offset of about two decades.

approaches (direct measurement and extrapolation) compare well when both can be used. The temperature evolution of ξ_d, normalized by its value at the onset temperature $\xi_0 = \xi_d(T_o)$, is shown in Fig. 3(a). After a fast transient at high temperature, we observe that the characteristic dynamic length scale is well described by an Arrhenius form, $\xi_d/\xi_0 \sim \exp(E_d/T)$, with $E_d \approx 0.13$, leading to an overall increase of a factor 4 between T_o and T_g in $2d$. Our estimate for ξ_d compares very well, but extends to lower T, the evolution of the average chord length reported for the same two-dimensional model [30]. Given the modest evolution of ξ_d, other functional forms are presumably possible.

We now compare our findings with earlier work. The good agreement with the determination of $z(T)$ from the average chord length measured in bulk simulations [30] not only confirms the validity of our strategy, but also shows that our approach is more flexible and much easier to implement over a broader temperature range.

Reference [18] proposes, among other measurements, a strategy to relate the extent of spatial relaxation events to their timescale. We can recast these results into a dynamic exponent, $z(T) = \alpha(1/T - 1/T_o)$ with a prefactor α that was evaluated for several models [18]. We explain this dictionary in Supplemental Material [36]. We compare these results to ours in Fig. 3(b). The two datasets deviate on two aspects. First, our data do not indicate that z vanishes at T_o. Second, our approach yields considerably larger values at low T: both sets yield $z \approx A/T$ at low T but with different prefactors. Measurements along the lines of [18] should be performed at lower T to better assess the nature of the reported difference in this regime.

A second comparison point with [18] is the characteristic length ξ_d. While we directly measured it, Keys *et al.* assume instead that relaxation events are triggered by localised excitations and estimate the average distance between them. We report tabulated values [18] in Fig. 3(a). While both datasets suggest a similar Arrhenius dependence, the corresponding energy scales E_d differ considerably. The very large correlation length predicted by Keys *et al.* at low T appears unrealistic [48]. We can conclude that either the numerical technique used before [18,19,21,22,50] to estimate the concentration of excitations is too crude, or that relaxation events are not simply due to localized excitations [30]. The very low T measurements in [50] do not show sign of a temperature crossover which could reconcile both families of measurements at low T.

Our results allow us to test the validity of the facilitation picture. Assuming that localized excitations relaxing with a characteristic timescale $\tau_{\rm ex}(T) \ll \tau_\alpha(T)$ can relax the entire system via dynamic facilitation, we arrive at

$$\tau_\alpha(T) \sim \tau_{\rm ex}\xi_d^z, \tag{6}$$

which represents the time it takes to grow a domain of size ξ_d from a localized excitation via dynamic facilitation. We test Eq. (6) using our direct, agnostic determinations of z, ξ_d, and τ_α. The results in Fig. 3(c) show that after a short transient at high T, τ_α becomes indeed proportional to ξ_d^z, with a prefactor of about 10^2 near T_g. This result suggests that the joint temperature evolution of $\xi_d(T)$ and $z(T)$ accounts for most of the 12-decade slowdown of the structural relaxation time $\tau_\alpha(T)$.

This conclusion is significant because it demonstrates the central role played by dynamic facilitation in controlling the dynamic slowdown of deeply supercooled liquids. At any temperature, dynamic facilitation "accelerates" the relaxation via the successive triggering of relaxation events [45], but since this process becomes increasingly

inefficient at low T (as captured by the rapid growth of z) the overall relaxation takes a longer time.

Our Letter thus identifies the two major contributors, $z(T)$ and $\xi_d(T)$, to the temperature dependence of $\tau_\alpha(T)$. While the interpretation of z is clear (it quantifies facilitation), our approach does not explain the evolution of $\xi_d(T)$ shown in Fig. 3(a), and this should be the subject of future studies. Combining the asymptotic Arrhenius evolution of ξ_d to the $1/T$ dependence of z found numerically provides an expression for the relaxation time:

$$\tau_\alpha \sim \xi_d^z \sim \exp\left(\frac{E_d A}{T^2}\right), \tag{7}$$

which is the parabolic Bässler law [51]. While [18] arrived at a similar functional form, we noted above that our determinations of E_d and A differ quantitatively, even if the products $E_d A$ in Eq. (7) appear very close to those reported in Ref. [18], as seen in Fig. 3(c).

The proposed slab geometry allows us to quantify how fast mobile regions spread to immobile ones with no assumption about the underlying microscopic mechanism. We can, however, test the specific modeling of facilitation of [10] which assumes that local elasticity is responsible for dynamic facilitation. As noted recently in thin polymer films [15], the slab geometry yields an algebraic gradient of elastic moduli, thus leading to algebraic dynamic profiles. We have tested this model by measuring spatial profiles of the Debye-Waller factor (mean-squared displacement at short times, known to strongly correlate with the shear modulus), and found rapid (nonalgebraic) convergence to the bulk value (see Supplemental Material [36]), in agreement with earlier results [52]. There is thus no correlation between elasticity and dynamic profiles, which are also found to converge exponentially (not algebraically) to the bulk behavior [recall Eq. (5)]. Together with [52], our data do not follow the analytic description of Ref. [10]. It would be interesting to analyse thermal elastoplastic models [13] in slab geometries. Although more limited, our results also suggest that the rugosity of the dynamic profiles decreases at low temperatures (see Supplemental Material [36]). This is in agreement with earlier numerical findings [30,53,54], but differs from hierarchical kinetically constrained models [24] and geometries found in elastoplastic models [13].

In conclusion, we introduced a computational scheme to quantify the role of dynamic facilitation in the relaxation dynamics of deeply supercooled liquids, which demonstrates a strongly subdiffusive and temperature dependent spatial spreading of relaxation events. A first future task is to expand these studies to a broader range of models to validate the generality of our findings. Our results also suggest that extending the approach of [18] to lower temperatures would be instructive. Future work should elucidate the microscopic mechanisms giving rise to the particular temperature dependence of the dynamic exponent $z(T)$. Finally, it is unclear how these results can be reconciled with the idea that dynamics proceeds via cooperative activated events stemming from static configurational fluctuations [55–57]. Overall, our Letter considerably sharpens the set of questions to be addressed in order to fully elucidate the nature of the structural relaxation in supercooled liquids near the glass transition.

We thank G. Biroli, J.-P. Bouchaud, J. Kurchan, and G. Tarjus for discussions. This work was funded through ANR (the French National Research Agency) under the Investissements d'avenir programme with the reference ANR-16-IDEX-0006. It was also supported by a grant from the Simons Foundation (No. 454933, L. B.), and by a Visiting Professorship from the Leverhulme Trust (VP1-2019-029, L. B.).

*Corresponding author: ludovic.berthier@umontpellier.fr

[1] M. D. Ediger, C. A. Angell, and S. R. Nagel, Supercooled liquids and glasses, J. Phys. Chem. **100**, 13200 (1996).
[2] M. D. Ediger, Spatially heterogeneous dynamics in supercooled liquids, Annu. Rev. Phys. Chem. **51**, 99 (2000).
[3] P. G. Debenedetti and F. H. Stillinger, Supercooled liquids and the glass transition, Nature (London) **410**, 259 (2001).
[4] L. Berthier and G. Biroli, Theoretical perspective on the glass transition and amorphous materials, Rev. Mod. Phys. **83**, 587 (2011).
[5] R. G. Palmer, D. L. Stein, E. Abrahams, and P. W. Anderson, Models of hierarchically constrained dynamics for glassy relaxation, Phys. Rev. Lett. **53**, 958 (1984).
[6] G. H. Fredrickson and H. C. Andersen, Kinetic Ising model of the glass transition, Phys. Rev. Lett. **53**, 1244 (1984).
[7] J. Jäckle and S. Eisinger, A hierarchically constrained kinetic Ising model, Z. Phys. B Condens. Matter **84**, 115 (1991).
[8] D. Chandler and J. P. Garrahan, Dynamics on the way to forming glass: Bubbles in space-time, Annu. Rev. Phys. Chem. **61**, 191 (2010).
[9] X. Xia and P. G. Wolynes, Microscopic theory of heterogeneity and nonexponential relaxations in supercooled liquids, Phys. Rev. Lett. **86**, 5526 (2001).
[10] S. Mirigian and K. S. Schweizer, Unified theory of activated relaxation in liquids over 14 decades in time, J. Phys. Chem. Lett. **4**, 3648 (2013).
[11] S. S. Schoenholz, E. D. Cubuk, D. M. Sussman, and A. J. Liu, A structural approach to relaxation in glassy liquids, Nat. Phys. **12**, 469 (2016).
[12] T. Speck, Dynamic facilitation theory: A statistical mechanics approach to dynamic arrest, J. Stat. Mech. (2019) 084015.
[13] M. Ozawa and G. Biroli, Elasticity, facilitation, and dynamic heterogeneity in glass-forming liquids, Phys. Rev. Lett. **130**, 138201 (2023).
[14] A. Tahaei, G. Biroli, M. Ozawa, M. Popović, and M. Wyart, Scaling description of dynamical heterogeneity and avalanches of relaxation in glass-forming liquids, Phys. Rev. X **13**, 031034 (2023).

[15] A. Ghanekarade, A. D. Phan, K. S. Schweizer, and D. S. Simmons, Signature of collective elastic glass physics in surface-induced long-range tails in dynamical gradients, Nat. Phys. **19**, 800 (2023).
[16] M. Vogel and S. C. Glotzer, Spatially heterogeneous dynamics and dynamic facilitation in a model of viscous silica, Phys. Rev. Lett. **92**, 255901 (2004).
[17] M. N. J. Bergroth, M. Vogel, and S. C. Glotzer, Examination of dynamic facilitation in molecular dynamics simulations of glass-forming liquids, J. Phys. Chem. B **109**, 6748 (2005).
[18] A. S. Keys, L. O. Hedges, J. P. Garrahan, S. C. Glotzer, and D. Chandler, Excitations are localized and relaxation is hierarchical in glass-forming liquids, Phys. Rev. X **1**, 021013 (2011).
[19] S. Gokhale, K. Hima Nagamanasa, R. Ganapathy, and A. Sood, Growing dynamical facilitation on approaching the random pinning colloidal glass transition, Nat. Commun. **5**, 4685 (2014).
[20] R. N. Chacko, F. P. Landes, G. Biroli, O. Dauchot, A. J. Liu, and D. R. Reichman, Elastoplasticity mediates dynamical heterogeneity below the mode coupling temperature, Phys. Rev. Lett. **127**, 048002 (2021).
[21] M. Isobe, A. S. Keys, D. Chandler, and J. P. Garrahan, Applicability of dynamic facilitation theory to binary hard disk systems, Phys. Rev. Lett. **117**, 145701 (2016).
[22] M. R. Hasyim and K. K. Mandadapu, A theory of localized excitations in supercooled liquids, J. Chem. Phys. **155**, 044504 (2021).
[23] P. Sollich and M. R. Evans, Glassy time-scale divergence and anomalous coarsening in a kinetically constrained spin chain, Phys. Rev. Lett. **83**, 3238 (1999).
[24] L. Berthier and J. P. Garrahan, Numerical study of a fragile three-dimensional kinetically constrained model, J. Phys. Chem. B **109**, 3578 (2005).
[25] C. Donati, S. C. Glotzer, and P. H. Poole, Growing spatial correlations of particle displacements in a simulated liquid on cooling toward the glass transition, Phys. Rev. Lett. **82**, 5064 (1999).
[26] N. Lačević, F. W. Starr, T. B. Schrøder, and S. C. Glotzer, Spatially heterogeneous dynamics investigated via a time-dependent four-point density correlation function, J. Chem. Phys. **119**, 7372 (2003).
[27] C. Toninelli, M. Wyart, L. Berthier, G. Biroli, and J.-P. Bouchaud, Dynamical susceptibility of glass formers: Contrasting the predictions of theoretical scenarios, Phys. Rev. E **71**, 041505 (2005).
[28] S. Karmakar, C. Dasgupta, and S. Sastry, Analysis of dynamic heterogeneity in a glass former from the spatial correlations of mobility, Phys. Rev. Lett. **105**, 015701 (2010).
[29] L. Berthier, G. Biroli, J.-P. Bouchaud, L. Cipelletti, and W. van Saarloos, *Dynamical Heterogeneities in Glasses, Colloids, and Granular Media* (Oxford University Press, New York, 2011).
[30] C. Scalliet, B. Guiselin, and L. Berthier, Thirty milliseconds in the life of a supercooled liquid, Phys. Rev. X **12**, 041028 (2022).
[31] M. D. Ediger, Perspective: Highly stable vapor-deposited glasses, J. Chem. Phys. **147**, 210901 (2017).
[32] C. Herrero, M. D. Ediger, and L. Berthier, Front propagation in ultrastable glasses is dynamically heterogeneous, J. Chem. Phys. **159**, 114504 (2023).
[33] S. Léonard and P. Harrowell, Macroscopic facilitation of glassy relaxation kinetics: Ultrastable glass films with frontlike thermal response, J. Chem. Phys. **133**, 244502 (2010).
[34] A. Sepúlveda, S. F. Swallen, and M. D. Ediger, Manipulating the properties of stable organic glasses using kinetic facilitation, J. Chem. Phys. **138**, 12A517 (2013).
[35] C. Herrero, C. Scalliet, M. D. Ediger, and L. Berthier, Two-step devitrification of ultrastable glasses, Proc. Natl. Acad. Sci. U.S.A. **120**, e2220824120 (2023).
[36] See Supplemental Material at http://link.aps.org/supplemental/10.1103/PhysRevLett.132.258201 for additional descriptions of C. References [37–40] are cited therein.
[37] M. Ozawa, C. Scalliet, A. Ninarello, and L. Berthier, Does the Adam-Gibbs relation hold in simulated supercooled liquids?, J. Chem. Phys. **151**, 084504 (2019).
[38] L. Larini, A. Ottochian, C. De Michele, and D. Leporini, Universal scaling between structural relaxation and vibrational dynamics in glass-forming liquids and polymers, Nat. Phys. **4**, 42 (2008).
[39] E. Flenner and G. Szamel, Fundamental differences between glassy dynamics in two and three dimensions, Nat. Commun. **6**, 7392 (2015).
[40] B. Illing, S. Fritschi, H. Kaiser, C. L. Klix, G. Maret, and P. Keim, Mermin-Wagner fluctuations in 2D amorphous solids, Proc. Natl. Acad. Sci. U.S.A. **114**, 1856 (2017).
[41] L. Berthier, P. Charbonneau, D. Coslovich, A. Ninarello, M. Ozawa, and S. Yaida, Configurational entropy measurements in extremely supercooled liquids that break the glass ceiling, Proc. Natl. Acad. Sci. U.S.A. **114**, 11356 (2017).
[42] L. Berthier, P. Charbonneau, A. Ninarello, M. Ozawa, and S. Yaida, Zero-temperature glass transition in two dimensions, Nat. Commun. **10**, 1508 (2019).
[43] A. Ninarello, L. Berthier, and D. Coslovich, Models and algorithms for the next generation of glass transition studies, Phys. Rev. X **7**, 021039 (2017).
[44] L. Berthier, E. Flenner, C. J. Fullerton, C. Scalliet, and M. Singh, Efficient swap algorithms for molecular dynamics simulations of equilibrium supercooled liquids, J. Stat. Mech. (2019) 064004.
[45] B. Guiselin, C. Scalliet, and L. Berthier, Microscopic origin of excess wings in relaxation spectra of supercooled liquids, Nat. Phys. **18**, 468 (2022).
[46] W. Kob, S. Roldán-Vargas, and L. Berthier, Non-monotonic temperature evolution of dynamic correlations in glass-forming liquids, Nat. Phys. **8**, 164 (2012).
[47] L. Berthier and J.-P. Bouchaud, Geometrical aspects of aging and rejuvenation in the Ising spin glass: A numerical study, Phys. Rev. B **66**, 054404 (2002).
[48] C. Dalle-Ferrier, C. Thibierge, C. Alba-Simionesco, L. Berthier, G. Biroli, J.-P. Bouchaud, F. Ladieu, D. L'Hôte, and G. Tarjus, Spatial correlations in the dynamics of glass-forming liquids: Experimental determination of their temperature dependence, Phys. Rev. E **76**, 041510 (2007).

[49] L. Berthier and M. D. Ediger, How to "measure" a structural relaxation time that is too long to be measured?, J. Chem. Phys. **153** (2020).
[50] L. Ortlieb, T. S. Ingebrigtsen, J. E. Hallett, F. Turci, and C. P. Royall, Probing excitations and cooperatively rearranging regions in deeply supercooled liquids, Nat. Commun. **14**, 2621 (2023).
[51] H. Bässler, Viscous flow in supercooled liquids analyzed in terms of transport theory for random media with energetic disorder, Phys. Rev. Lett. **58**, 767 (1987).
[52] D. M. Sussman, S. S. Schoenholz, E. D. Cubuk, and A. J. Liu, Disconnecting structure and dynamics in glassy thin films, Proc. Natl. Acad. Sci. U.S.A. **114**, 10601 (2017).
[53] P. Das and S. Sastry, Crossover in dynamics in the Kob-Andersen binary mixture glass-forming liquid, J. Non-Crystalline Solids: X **14**, 100098 (2022).
[54] G. Jung, G. Biroli, and L. Berthier, Predicting dynamic heterogeneity in glass-forming liquids by physics-inspired machine learning, Phys. Rev. Lett. **130**, 238202 (2023).
[55] T. R. Kirkpatrick, D. Thirumalai, and P. G. Wolynes, Scaling concepts for the dynamics of viscous liquids near an ideal glassy state, Phys. Rev. A **40**, 1045 (1989).
[56] J.-P. Bouchaud and G. Biroli, On the Adam-Gibbs-Kirkpatrick-Thirumalai-Wolynes scenario for the viscosity increase in glasses, J. Chem. Phys. **121**, 7347 (2004).
[57] L. Berthier, Self-induced heterogeneity in deeply supercooled liquids, Phys. Rev. Lett. **127**, 088002 (2021).